J|A|C|S
ARTICLES
Published on Web 12/15/2001

Calorimetric and Structural Studies of 1,2,3-Trisubstituted Cyclopropanes as Conformationally Constrained Peptide Inhibitors of Src SH2 Domain Binding

James P. Davidson,[‡] Olga Lubman,[§] Thierry Rose,[§] Gabriel Waksman,*[,§] and Stephen F. Martin*[,‡]

Contribution from the Department of Chemistry and Biochemistry and The Institute of Cellular and Molecular Biology, The University of Texas, Austin, Texas 78712, and Department of Biochemistry and Molecular Biophysics, Washington University School of Medicine, St. Louis, Missouri 63110

Received July 17, 2001

Abstract: Isothermal titration calorimetry and X-ray crystallography have been used to determine the structural and thermodynamic consequences associated with constraining the pTyr residue of the pYEEI ligand for the Src Homology 2 domain of the Src kinase (Src SH2 domain). The conformationally constrained peptide mimics that were used are cyclopropane-derived isosteres whereby a cyclopropane ring substitutes to the *N*-Cα-Cβ atoms of the phosphotyrosine. Comparison of the thermodynamic data for the binding of the conformationally constrained peptide mimics relative to their equivalent flexible analogues as well as a native tetrapeptide revealed an entropic advantage of 5−9 cal mol^{-1} K^{-1} for the binding of the conformationally constrained ligands. However, an unexpected drop in enthalpy for the binding of the conformationally constrained ligands relative to their flexible analogues was also observed. To evaluate whether these differences reflected conformational variations in peptide binding modes, we have determined the crystal structure of a complex of the Src SH2 domain bound to one of the conformationally constrained peptide mimics. Comparison of this new structure with that of the Src SH2 domain bound to a natural 11-mer peptide (Waksman et al. *Cell* **1993**, *72*, 779−790) revealed only very small differences. Hence, cyclopropane-derived peptides are excellent mimics of the bound state of their flexible analogues. However, a rigorous analysis of the structures and of the surface areas at the binding interface, and subsequent computational derivation of the energetic binding parameters, failed to predict the observed differences between the binding thermodynamics of the rigidified and flexible ligands, suggesting that the drop in enthalpy observed with the conformationally constrained peptide mimic arises from sources other than changes in buried surface areas, though the exact origin of the differences remains unclear.

Introduction

Oligopeptides have been commonly used as lead compounds to design ligands or drugs with high affinity and specificity for a particular binding site. A number of strategies have been developed to achieve this goal, and one that has proven particularly meritorious involves incorporating conformational constraints into the oligopeptide. This approach allows the topography of the binding site and the biologically active conformation, or the bound structure, of the ligand to be explored,[1−7] and ligands exhibiting increased affinity or specificity for the receptor or enzyme active site can be identified. One of the assumed benefits of preorganizing a ligand into the biologically active conformation is that this will give rise to an entropic advantage in the binding event. This favorable entropy of binding would eventuate in tighter binding, provided there were no enthalpic penalties that arose from a loss of attractive interactions or the introduction of unfavorable steric interactions in the complex.

A survey of the vast majority of peptide mimics reveals that most are dedicated to controlling backbone organization; few are capable of orienting the amino acid side chains, which contribute critical recognition elements for binding and specificity.[8−12] Thus, there is a general need for peptide replacements that predictably constrain both the peptide back-

* To whom correspondence should be addressed. G.W.: phone, (314) 362-4562; fax, (314) 362-7183; e-mail, waksman@biochem.wustl.edu. S.F.M.: phone, (512) 471-3915; fax, (512) 471-4180; e-mail, sfmartin@mail.utexas.edu.

‡ The University of Texas.

§ Washington University School of Medicine.

(1) Babine, R. E.; Bender, S. L. *Chem. Rev.* **1997**, *97*, 1359−1472.
(2) Ball, J. B.; Alewood, P. F. *J. Mol. Recognit.* **1990**, *3*, 55−64.
(3) Giannis, A.; Kolter, T. *Angew. Chem., Int. Ed. Engl.* **1993**, *32*, 1244−1267.
(4) Gibson, S. E.; Guillo, N.; Tozer, M. J. *Tetrahedron* **1999**, *55*, 585−615.
(5) Liskamp, R. M. J. *Recl. Trav. Chim. Pays-Bas* **1994**, *113*, 1−19.
(6) Olson, G. L.; Bolin, D. R.; Bonner, M. P.; Bos, M.; Cook, C. M.; Fry, D. C.; Graves, B. J.; Hatada, M.; Hill, D. E.; et al. *J. Med. Chem.* **1993**, *36*, 3039−3049.
(7) Patani, G. A.; LaVoie, E. J. *Chem. Rev.* **1996**, *96*, 3147−3176.
(8) Boumendjel, A.; Roberts, J. C.; Hu, E.; Pallai, P. V.; Rebek, J., Jr. *J. Org. Chem.* **1996**, *61*, 4434−4438.
(9) Chen, L.; Trilles, R. V.; Tilley, J. W. *Tetrahedron Lett.* **1995**, *36*, 8715−8718.
(10) Hagihara, M.; Anthony, N. J.; Stout, T. J.; Clardy, J.; Schreiber, S. L. *J. Am. Chem. Soc.* **1992**, *114*, 6568−6570.

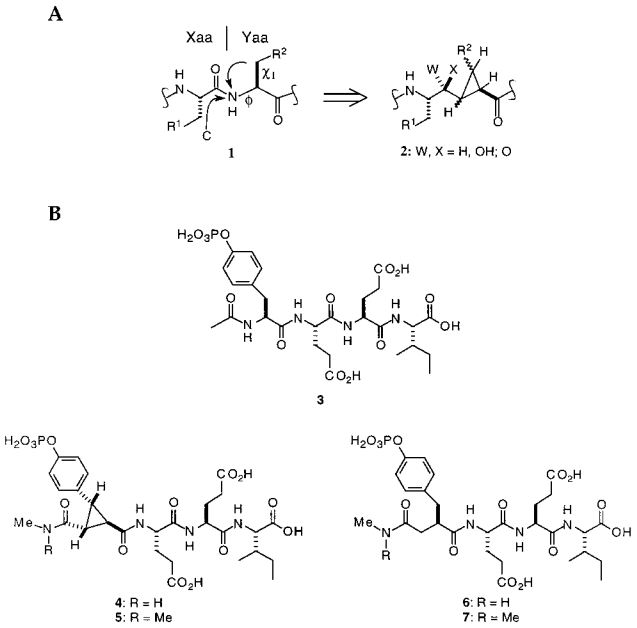

Figure 1. Conceptual design of 1,2,3-trisubstituted cyclopropane replacements of peptides (A) and formulas of the peptides and pseudopeptides used in this study (B). In (A), the rotors constrained by the substitution are indicated by ϕ and χ_1. In (B), compounds **3**−**7** are shown.

bone and the side chains in orientations that correspond to the biologically active conformation of the peptide. Toward this end, we designed a novel class of cyclopropane-derived dipeptide isosteres related to **2** (Figure 1A).[13] The cyclopropane ring in **2** replaces two atoms in the peptide backbone of the native dipeptide **1** as well as the β-carbon of the amino acid (Yaa) being replaced (Figure 1A). These unique replacements were designed to orient both the peptide backbone and the amino acid side chain by varying the stereochemistry on the cyclopropane ring.

To evaluate the efficacy of such replacements in biological systems, cyclopropane-derived isosteres related to **2** were introduced into inhibitors of renin, HIV-1 protease, matrix metalloproteinases, and Ras farnesyltransferase, as well as enkephalin analogues and fibrinogen receptor antagonists.[14−20] These studies generally established the viability of introducing trisubstituted cyclopropanes into biologically active analogues of peptides and provided evidence that these replacements could be used to probe the topography of the binding site. High affinity ligands were identified in a number of cases; however, in contrast to original expectations, the potency of the conformationally constrained ligands were at best equal, not superior, to their flexible peptide counterparts. Hence, the primary goal of preparing tighter binding pseudopeptides through conformational constraint was not achieved, and the fundamental question at this juncture was "Why?" Did the introduction of the cyclopropane ring into the inhibitors not result in the expected entropic advantage, or did unfavorable enthalpic factors such as loss of binding contacts or steric interactions override the entropic gains, thereby resulting in a similar free energy of binding? Because there have been no studies that directly assess the thermodynamic consequences ($\Delta G°$, $\Delta H°$, and $\Delta S°$) of preorganizing a ligand into its biologically active conformation, we designed a set of calorimetric and structural experiments to evaluate the consequences of introducing this localized conformational constraint into pseudopeptides.

After considering a number of possibilities, we concluded that complexes of Src Homology 2 (SH2) domains with phosphotyrosyl-derived ligands would constitute an excellent biological system in which to probe the effects of structure and energetics of binding. SH2 domains are small protein domains containing ~100 amino acids that play critical roles in a variety of signal transduction pathways.[21−23] These domains specifically bind to tyrosine-phosphorylated sites, thereby facilitating recruitment of SH2 domain-containing proteins to these sites.[24] The design of potent and selective SH2 domain-binding inhibitors that selectively target these signaling processes has been of keen interest in the pharmaceutical industry.[25,26] One notable success in this area has been the design of compounds that are selective for the SH2 domain of the Src kinase (Src SH2 domain) and that selectively inhibit bone resorption in vivo.[27−29]

The phosphotyrosine-containing tetrapeptide Ac-pTyr-Glu-Glu-Ile-OH (pYEEI) (**3**) is a well-known antagonist of the SH2 domains of the Src family of kinases.[30] Examination of known three-dimensional structures of pTyr ligands in complex with Src family SH2 domains[31−33] revealed that the cyclopropane-derived analogues **4** and **5**, which are conformationally constrained derivatives of **3**, were well suited to probe thermody-

(11) Janetka, J. W.; Raman, P.; Satyshur, K.; Flentke, G.; Rich, D. H. *J. Am. Chem. Soc.* **1997**, *119*, 441−442.
(12) Smith, A. B., III; Guzman, M. C.; Sprengeler, P. A.; Keenan, T. P.; Holcomb, R. C.; Wood, J. L.; Carroll, P. J.; Hirschmann, R. *J. Am. Chem. Soc.* **1994**, *116*, 9947−9962.
(13) Martin, S. F.; Austin, R. E.; Oalmann, C. J. *Tetrahedron Lett.* **1990**, *31*, 4731−4734.
(14) Hillier, M. C.; Davidson, J. P.; Martin, S. F. *J. Org. Chem.* **2001**, *66*, 1657−1671.
(15) Martin, S. F.; Austin, R. E.; Oalmann, C. J.; Baker, W. R.; Condon, S. L.; deLara, E.; Rosenberg, S. H.; Spina, K. P.; Stein, H. H.; Cohen, J.; Kleinert, H. D. *J. Med. Chem.* **1992**, *35*, 1710−1721.
(16) Martin, S. F.; Dorsey, G. O.; Gane, T.; Hillier, M. C.; Kessler, H.; Baur, M.; Mathae, B.; Erickson, J. W.; Bhat, T. N.; Munshi, S.; Gulnik, S. V.; Topol, I. A. *J. Med. Chem.* **1998**, *41*, 1581−1597.
(17) Martin, S. F.; Dwyer, M. P.; Hartmann, B.; Knight, K. S. *J. Org. Chem.* **2000**, *65*, 1305−1318.
(18) Martin, S. F.; Oalmann, C. J.; Liras, S. *Tetrahedron* **1993**, *49*, 3521−3532.
(19) Baker, W. R.; Jae, H. S.; Martin, S. F.; Condon, S. L.; Stein, H. H.; Cohen, J.; Kleinert, H. D. *Bioorg. Med. Chem. Lett.* **1992**, *2*, 1405−1410.
(20) Bovy, P. R.; Tjoeng, F. S.; Rico, J. G.; Rogers, T. E.; Lindmark, R. J.; Zablocki, J. A.; Garland, R. B.; McMackins, D. E.; Dayringer, H.; et al. *Bioorg. Med. Chem.* **1994**, *2*, 881−895.
(21) Cantley, L. C.; Auger, K. R.; Carpenter, C.; Duckworth, B.; Graziani, A.; Kapeller, R.; Soltoff, S. *Cell* **1991**, *64*, 281−302.
(22) Pawson, T.; Schlessinger, J. *Curr. Biol.* **1993**, *3*, 434−442.
(23) Sadowski, I.; Stone, J. C.; Pawson, T. *Mol. Cell. Biol.* **1986**, *6*, 4396−4408.
(24) Pawson, T.; Scott, J. D. *Science* **1997**, *278*, 2075−2080.
(25) Brugge, J. S. *Science* **1993**, *260*, 918−919.
(26) Sawyer, T. K. *Biopolymers* **1998**, *47*, 243−261.
(27) Charifson, P. S. S., L. M.; Rocque, W.; Hummel, C. W.; Jordan, S. R.; Mohr, C.; Pacofsky, G. J.; Peel, M. J.; Rodriguez, M.; Sternback, D. D.; Consler, T. G. *Biochemistry* **1997**, *36*, 6283−6293.
(28) Shakespeare, W.; Yang, M.; Bohacek, R.; Cerasoli, F.; Stebbins, K.; Sundaramoorthi, R.; Azimioara, M.; Vu, C.; Pradeepan, S.; Metcalf, C.; Haraldson, C.; Merry, T.; Dalgarno, D.; Narula, S.; Hatada, M.; Lu, X. D.; van Schravendijk, M. R.; Adams, S.; Violette, S.; Smith, J.; Guan, W.; Bartlett, C.; Herson, J.; Iuliucci, J.; Weigele, M.; Sawyer, T. *Proc. Natl. Acad. Sci. U.S.A.* **2000**, *97*, 9373−9378.
(29) Violette, S. M.; Shakespeare, W. C.; Bartlett, C.; Guan, W.; Smith, J. A.; Rickles, R. J.; Bohacek, R. S.; Holt, D. A.; Baron, R.; Sawyer, T. K. *Chem. Biol.* **2000**, *7*, 225−235.
(30) Zhou, S. Y.; Shoelson, S. E.; Chaudhuri, M.; Gish, G.; Pawson, T.; Haser, W. G.; King, F.; Roberts, T.; Ratnofsky, S.; Lechleider, R. J.; Neel, B. G.; Birge, R. B.; Fajardo, J. E.; Chou, M. M.; Hanafusa, H.; Schaffhausen, B.; Cantley, L. C. *Cell* **1993**, *72*, 767−778.
(31) Waksman, G.; Kominos, D.; Robertson, S. C.; Pant, N.; Baltimore, D.; Birge, R. B.; Cowbrun, D.; Hanafusa, H.; Mayer, B. J.; Overduin, M.; Resh, M. D.; Rios, C. B.; Silverman, L.; Kuryian, J. *Nature* **1992**, *358*, 646−653.
(32) Waksman, G.; Shoelson, S. E.; Pant, N.; Cowburn, D.; Kuriyan, J. *Cell* **1993**, *72*, 779−790.
(33) Eck, M. J.; Shoelson, S. E.; Harrison, S. C. *Nature* **1993**, *362*, 87−91.

namic and structural consequences of the cyclopropane-derived conformational constraint. Because **4** and **5** lack the tyrosine amide nitrogen atom of **3**, the pseudopeptides **6** and **7** were identified as the necessary flexible controls. Compounds **4**−**7** were prepared by standard synthetic methods and initially screened in competitive binding experiments to evaluate the relative affinities of these compounds for the SH2 domain of the Src family kinase Lck (Lck SH2 domain).[34] These results indicated that both of the constrained ligands **4** and **5** bound to the SH2 domain with higher affinity than their flexible counterparts **6** and **7**, but the energetic differences were small (<0.6 kcal mol^{-1}); the native tetrapeptide **3** and the synthetic pseudopeptide **4** were equipotent.

The observation that the constrained ligands **4** and **5** bound to the Lck SH2 domain better than **6** and **7**, respectively, supported the original premise that introducing a conformational constraint enhanced binding. Elucidating the energetic origin of these differences, however, required calorimetric studies to determine the complete thermodynamic profiles ($\Delta\Delta G°$, $\Delta\Delta H°$, $\Delta\Delta S°$, and $\Delta\Delta C_p$) for forming the different protein−ligand complexes. Unfortunately, some of the regions of the Lck SH2 domain that are intimately involved in phosphotyrosine binding have been shown to undergo significant conformational changes upon binding of phosphotyrosine-containing ligands similar to **3**−**7**.[35] Because such structural changes would complicate the interpretation of the calorimetric data, we turned our attention to the Src SH2 domain, which was known not to undergo these conformational changes upon binding.[31,32,36] The Src SH2 domain has been the subject of numerous structural and calorimetric studies that have led to a detailed knowledge of the binding energetics ($\Delta G°$, $\Delta H°$, $\Delta S°$, and ΔC_p) associated with these protein−ligand interactions, thus providing a broad knowledge base from which to launch our investigations.[27,31,32,36−44]

In this account, we report the thermodynamic profiles for the binding of the conformationally constrained phosphotyrosyl peptides **4** and **5**, their flexible analogues **6** and **7**, and the tetrapeptide **3** to the Src SH2 domain. These profiles are analyzed in the context of the crystal structures of the known complex of the Src SH2 domain, an 11-mer natural tyrosyl phosphopeptide containing the pYEEI motif,[32] and a new structure of the same SH2 domain bound to the conformationally constrained pseudopeptide **4**.

Experimental Section

Protein Expression and Purification. The Src SH2 domain was expressed and purified as described previously by Waksman et al.[31,36] The purity of the resulting material was assessed to be >98% by SDS-PAGE. The protein was then dialyzed twice (24 h, 4 °C, 2 L of buffer) against the standard calorimetry buffer (20 mM HEPES, pH 7.3, 1 mM β-mercaptoethanol, 1 mM EDTA, 100 mM NaCl). The published extinction coefficient of 14 700 M^{-1} cm^{-1} was used to determine the final protein concentrations for the calorimetry experiments.[36] Typical yields for this purification procedure were 40−50 mg/L of culture.

Syntheses of Phosphotyrosines 3−7. Compounds **3**−**7** were synthesized as reported previously by Davidson and Martin,[34] and complete experimental details for the syntheses of **3**−**7** are included in the Supporting Information. The experimentally determined extinction coefficient of 775 M^{-1} cm^{-1} at 268 nm was used to determine the final ligand concentrations after dissolution in the standard calorimetry buffer, pH adjustment, and filtration.

Isothermal Titration Calorimetry. Calorimetry experiments were performed with an MCS titration calorimeter obtained from Microcal Inc. (Northhampton, MA) as described in detail by Wiseman.[45] Protein and ligand solutions were degassed with stirring under reduced pressure for 15 min prior to experiments. For a typical titration experiment, 50−75 μM Src SH2 domain was placed in the 1.35 mL reaction cell, and the 0.6−0.8 mM phosphotyrosine mimic was loaded into the 250 μL injection syringe. Phosphotyrosine mimics were injected in 8−12 μL increments. At least five injections were typically performed after saturation was observed. All values in the results section are the result of at least three independent titration experiments. The data for each titration were collected by the ORIGIN software provided with the calorimeter, and the titration curves were fit using the same software to give $\Delta H°$ and K_a. For each ligand, at each experimental temperature, a blank was run where ligand was injected into buffer alone to establish the nonzero heat of dilution for the ligand. This heat was subtracted from the raw titration data prior to fitting. The integrated data from all experiments fit the single-site binding model with the stoichiometry of binding being between 0.95 and 1.15 for all titrations. The *c* value, defined as the product of the association constant K_a and the macromolecule concentration *M*, was within the range of 1−1000, as per the manufacturer's recommendations for the determination of accurate binding constants, for all experiments.[45]

Crystallization and Data Collection. Crystals of the Src SH2 domain complexed with compound **4** were grown by the hanging drop method with 40 mg mL^{-1} solutions of 1:2 molar ratio of protein to compound complex equilibrated against a reservoir containing 50% MPD and 0.1 M HEPES, pH 8.0. The crystals diffracted to a resolution of 1.9 Å in the laboratory setting (Rigaku Raxis IV image plate mounted on a Rigaku RU200 rotating anode generator). A complete data set to a resolution of 1.9 Å (Table 1) was collected using a single crystal with an oscillation range of 1.0° and an exposure time of 30 min/frame. Crystals were in the orthorhombic space group $P2_12_12_1$, with cell dimensions $a = 58.3$ Å, $b = 56.5$ Å, and $c = 69.3$ Å, and two molecules per asymmetric unit. All X-ray diffraction data were reduced using the program DENZO and scaled using SCALEPACK.[46]

Structure Determination and Refinement. The structure of the Src SH2 domain−compound **4** complex was solved by the molecular replacement method, using the program AMoRe.[47] The search model consisted of the coordinates of the Src SH2 domain from the refined structure of the wild-type Src SH2 domain bound to the 11-mer peptide EPQpYEEIPIYL (RCSB ID code 1sps)[32] with the peptide and water molecules omitted. The molecular replacement search yielded a clear solution peak with high correlation coefficient (45.8) and low R-factor (40.6%). The structure was refined using simulated annealing in torsional angle space using the program CNS.[48,49] Model inspection and manual rebuilding were carried out in simulated annealing omit maps using the program O.[50,51] After bulk solvent correction, the refinement converged to a final R-factor of 23.6% and free R-factor of

(34) Davidson, J. P.; Martin, S. F. *Tetrahedron Lett.* **2000**, *41*, 9459−9464.
(35) Tong, L.; Warren, T. C.; Lukas, S.; Schembri-King, J.; Betageri, R.; Proudfood, J. R.; Jakes, S. *J. Biol. Chem.* **1998**, *273*, 20238−20242.
(36) Bradshaw, J. M.; Grucza, R. A.; Ladbury, J. E.; Waksman, G. *Biochemistry* **1998**, *37*, 9083−9090.
(37) Bradshaw, J. M.; Mitaxov, V.; Waksman, G. *J. Mol. Biol.* **2000**, *299*, 521−535.
(38) Bradshaw, J. M.; Waksman, G. *Biochemistry* **1998**, *37*, 15400−15407.
(39) Bradshaw, J. M.; Waksman, G. *Biochemistry* **1999**, *38*, 5147−5154.
(40) Bradshaw, J. M.; Mitaxov, V.; Waksman, G. *J. Mol. Biol.* **1999**, *293*, 971−985.
(41) Grucza, R. A.; Bradshaw, J. M.; Futterer, K.; Waksman, G. *Med. Res. Rev.* **1999**, *19*, 273−293.
(42) Grucza, R. A.; Bradshaw, J. M.; Mitaxov, V.; Waksman, G. *Biochemistry* **2000**, *39*, 10072−10081.
(43) Henriques, D. A.; Ladbury, J. E.; Jackson, R. M. *Protein Sci.* **2000**, *9*, 1975−1985.
(44) Xu, R. X. W., M. J.; Davis, D. G.; Rink, M. J.; Willard, D. H.; Gampe, R. T. *Biochemistry* **1995**, *34*, 2107−2121.
(45) Brandts, J. F.; Wiseman, T.; Williston, S. *Anal. Biochem.* **1989**, *179*.
(46) Otwinowski, Z.; Minor, W. *Macromol. Crystallogr., Part A* **1997**, *276*, 307−326.
(47) Navaza, J. *Acta Crystallogr., Sect. A* **1994**, *50*, 157−163.

Table 1. Data Collection and Refinement Statistics

Data Collection

radiation	resolution	total/unique reflections	completeness[a] (%)	R_{sym} (%)[b]
Cu Kα	30−1.9 Å	101 439/18 121	97.0 (95.3)	0.031 (0.11)

Refinement

resolution (Å)	number of reflections[c]	total number of atoms[d]	R-factor/R_{free} (%)[e]	rms deviations[f]		
				bonds (A)	angles (deg)	B-values
30.0−1.9	16 124 (86.5/82.1%)	1873	23.6/26.7	0.013	1.8	1.2(main chain) 1.4(side chain)

[a] Completeness for $I/\sigma(I) > 1$, high-resolution shell (1.97−1.9 Å) in parentheses. [b] $R_{sym} = \sum|I - \langle I\rangle|/\sum I$, where I is the observed intensity, and $\langle I\rangle$ is the average intensity from multiple observations of symmetry related reflections; high resolution (1.97−1.9 Å) shell in parentheses. [c] Numbers reflect "working" set of reflections at $F/\sigma(F) > 2.0$, overall/last shell (1.97−1.9) completeness in parentheses. [d] Includes 189 water molecules. [e] R_{free} was calculated on the basis of 10% of the total number of reflections randomly omitted from the refinement. [f] Deviations from ideal bond lengths and angles and in B factors of bonded atoms.

26.7%. The refined structure contains 207 amino acids in the two protein molecules, two molecules of compound **4**, and 189 water molecules. Details on data collection and refinement statistics are presented in Table 1. The PDB entry code for this structure is 1IS0.

Structure-Based Thermodynamic Calculation. The protein−peptide binding thermodynamic parameters were calculated from changes in solvent-accessible surface areas (ΔASA) during intermolecular association according to the method of Baker and Murphy as applied to the Src SH2 domain−peptide interaction by Henriques et al.[43,52] The empirical binding energies were evaluated for compound **4** from the crystal structure of the two Src SH2 domain−compound **4** complexes present in the asymmetric unit of the crystals described herein. The structure of the Src SH2 domain complexes bound to compounds **3** and **6** were modeled from the structure of the Src SH2 domain cocrystallized with the 11-mer peptide EPQYEEIPIYL.[32] The asymmetric unit of these crystals contained three such complexes, and all three were used as starting point templates to build compounds **3** and **6** (program INSIGHTII, MSI, San Diego, CA). These models were optimized by a four-step protocol using the program Discover and the force field CFF91 (MSI, San Diego, CA) with no cut off and a dielectric constant fixed to $1 \times r$. Potential energy minimization was applied successively (1) to peptide side chains only, using 100 cycles of steepest descent minimization, (2) to peptide and protein side chains, using 1000 cycles of conjugate gradient minimization, (3) to all the peptide atoms and protein side chains, as in step 2, and (4) then to all atoms except the Src SH2 backbone atoms located 10 Å or more away from the peptide, as in step 2. Root mean square (rms) deviation calculations between final and starting models and stereochemistry validation using the program PROCHECK were systematically performed.[53]

ΔASAs were calculated using a 1.4 Å radius probe and the following definitions:

$$\Delta ASA_{total} = ASA_{Src\ SH2:peptide} - ASA_{Src\ SH2} - ASA_{peptide}$$

$$\Delta ASA = \Delta ASA_{polar} + \Delta ASA_{nonpolar}$$

$ASA_{Src\ SH2}$ is calculated from the structure of the complex where the ligand has been removed. The changes in heat capacity $\Delta C_{p,calc}$ were calculated from the area variations upon binding of the polar and nonpolar water accessible surfaces according to Baker and Murphy:[52]

$$\Delta C_{p,calc} = -0.26\Delta ASA_{polar} + 0.43\Delta ASA_{nonpolar}$$

The change in enthalpy $\Delta H°$ was evaluated at 60 °C using the following formula from Baker and Murphy:[52]

$$\Delta H°_{333K} = 29.19\Delta ASA_{polar} - 7.27\Delta ASA_{nonpolar}$$

and extrapolated at 25 °C using the following:

$$\Delta C_{p,calc} = (\Delta H°_{298K} - \Delta H°_{333K})/(333 - 298)$$

$$\Delta H°_{298K} = \Delta C_{p,calc}/(333 - 298) + \Delta H°_{333K}$$

The changes in entropy were calculated as the sum of the conformational entropy $\Delta S°_{conf}$, the association entropy $\Delta S°_{asso}$, and the solvation entropy $\Delta S°_{solv}$ defined as follows:

$$\Delta S°_{conf} = \sum_i^n(\Delta ASA_{SC,i}/ASA_{AXA-SC,i})S°_{BuEx} + \sum_i^n(\Delta ASA_{BB,i}/ASA_{AXA-BB,i})S°_{BB} + \sum_i^n(\Delta ASA_{BB,i}/ASA_{AXA-BB,i})S°_{Ex-U}$$

where $\Delta ASA_{SC,i}$ or $\Delta ASA_{BB,i}$ are the changes in ASA of the side chain or the backbone of residue i on binding. $ASA_{AXA-SC,i}$ or $ASA_{AXA-BB,i}$ are the ASA of the side chain or the backbone of residue i in an extended Ala-X-Ala tripeptide.[43,52] Values for the backbone entropy $S°_{BB}$ and $S°_{Ex-U}$ were from D'Aquino et al.,[54] and the values for side-chain entropy ($S°_{BuEx}$) were from Lee et al.[55]

$$\Delta S°_{asso} = -7.89\ \text{cal}\ K^{-1}\ \text{mol}^{-1}$$

$$\Delta S°_{solv} = \Delta C_{p,calc}\ \ln(298/385)$$

Finally the binding free energy was computed from $\Delta G° = \Delta H° - T\Delta S°$.

Results

Thermodynamic Profiles for Complexes of Src SH2 Domain with Compounds 3−7. Compounds **4**−**7** are peptide mimics that contain rigid structural replacements for the phosphotyrosine (pTyr). For example, compounds **4** and **5** contain a cyclopropane ring as a replacement for the *N*-Cα-C*β* atoms of the pTyr in the parent peptide compound **3**. In compounds **6** and **7**, the amide nitrogen of pTyr in compound

(48) Brunger, A. T.; Adams, P. D.; Clore, G. M.; DeLano, W. L.; Gros, P.; Grosse-Kunstleve, R. W.; Jiang, J. S.; Kuszewski, J.; Nilges, M.; Pannu, N. S.; Read, R. J.; Rice, L. M.; Simonson, T.; Warren, G. L. *Acta Crystallogr., Sect. D* **1998**, *54*, 905−921.
(49) Rice, L. M.; Brunger, A. T. *Proteins* **1994**, *19*, 277−290.
(50) Hodel, A.; Kim, S. H.; Brunger, A. T. *Acta Crystallogr., Sect. A* **1992**, *48*, 851−858.
(51) Jones, T. A.; Zou, J. Y.; Cowan, S. W.; Kjeldgaard, M. *Acta Crystallogr., Sect. A* **1991**, *47*, 110−119.
(52) Baker, B. M.; Murphy, K. P. *Methods Enzymol.* **1998**, *295*, 294−315.
(53) Laskowski, R. A.; Moss, D. S.; Thornton, J. M. *J. Mol. Biol.* **1993**, *231*, 1049−1067.
(54) D'Aquino, J. A.; Gomez, J.; Hilser, V. J.; Lee, K. H.; Amzel, L. M.; Freire, E. *Proteins* **1996**, *25*, 143−156.
(55) Lee, K. H.; Xie, D.; Freire, E.; Amzel, L. M. *Proteins* **1994**, *20*, 68−84.

Table 2. Thermodynamic Parameters Determined at 25 °C and Change in Heat Capacity Values[a]

compound	K_a	$\Delta G°_{obs}$ (kcal mol^{-1})	$\Delta H°_{obs}$ (kcal mol^{-1})	$\Delta S°_{obs}$ (cal mol^{-1} K^{-1})	$\Delta C_{p,obs}$ (cal mol^{-1} K^{-1})
3	4.1 ($\pm$0.1) $\times$ 10^6	-9.01 ± 0.01	-6.06 ± 0.05	9.9 ± 0.2	
4	1.0 ($\pm$0.1) $\times$ 10^7	-9.55 ± 0.07	-5.91 ± 0.04	17 ± 1	-225 ($\pm$9)
6	1.7 ($\pm$0.6) $\times$ 10^7	-9.8 ± 0.2	-7.33 ± 0.03	8.3 ± 0.5	-213 ($\pm$17)
5	6.3 ($\pm$0.6) $\times$ 10^6	-9.26 ± 0.06	-5.01 ± 0.05	14.3 ± 0.4	
7	1.4 ($\pm$0.1) $\times$ 10^7	-9.72 ± 0.06	-6.92 ± 0.09	9.4 ± 0.2	

[a] Errors represent the standard deviations between multiple measurements.

3 is substituted with a methylene, CH_2, group. The additional carbon−carbon bond in the pTyr replacements of **4** and **5** introduce conformational constraints that are absent in the more flexible succinate derivatives **6** and **7**. The other difference is that the *N*-terminal acetyl (CH_3CO-) group in **3** is replaced with a methyl amide (CH_3NHCO-) or dimethyl amide [$(CH_3)_2NCO-$] group (Figure 1B). Owing to their structural similarities, any observed differences in binding energetics for the constrained compounds **4** and **5** relative to the corresponding flexible counterparts **6** and **7** would be expected to result solely from the conformational constraints imposed by the cyclopropane ring.

The energetics of binding of compounds **3**−**7** were determined by isothermal titration calorimetry. The experimentally determined and calculated thermodynamic data for these compounds are summarized in Table 2. All compounds in this study bound to the Src SH2 domain at 25 °C with a favorable enthalpy ($\Delta H° < 0$) and favorable entropy ($\Delta S° > 0$) as shown in Table 2. This trend was expected on the basis of previous studies of SH2 domain−phosphopeptide interactions.[36,56,57] Each of the pseudopeptides **4**−**7** bound to the Src SH2 domain with slightly higher affinity than the parent tetrapeptide **3** (Table 2). Neither cyclopropane-containing compound **4** nor **5** exhibited a higher affinity than the flexible analogue **6** or **7**, respectively, as had been observed previously.[34] The tetrapeptide **3** binds with only a 0.5 kcal mol^{-1} less favorable free energy change than an 8-mer peptide having the sequence Ac-PQpYEEIPI-NH_2 under similar conditions.[36] Hence, residues beyond the pYEEI motif do not appear to make significant contributions to the binding free energy.[32]

The thermodynamic profiles for the binding of both cyclopropane-containing ligands **4** and **5** showed a significant entropic advantage ($\Delta\Delta S° = 5-9$ cal mol^{-1} K^{-1}) over the tetrapeptide **3** and their flexible analogues **6** and **7**. The favorable $\Delta\Delta S°$ corresponds approximately to that predicted for restricting two "rotors" (χ_1 and Φ in Figure 1A).[58,59] This result supports the hypothesis that the preorganization of a ligand in its active conformation does give rise to a favorable entropic contribution to binding. Both cyclopropane-containing compounds **4** and **5** bound to the SH2 domain with significantly less favorable enthalpies of binding ($\Delta\Delta H° = 1.4-1.9$ kcal mol^{-1} relative to their flexible analogues **6** and **7**). Thus, the introduction of the conformational constraint resulted in significant differences in both the enthalpy and the entropy changes of binding without effecting $\Delta G°$ significantly.

To probe whether incorporating the cyclopropane ring would contribute significantly to the hydrophobic interactions or the solvation−desolvation processes during complex formation, the changes in heat capacities ($\Delta C_{p,obs}$) for compounds **4** and **6** were determined.[60,61] Titrations were carried out at intervals of 5 °C at temperatures from 15 to 35 °C. When $\Delta H°_{obs}$ is plotted versus temperature (Figure 2), the plot is linear, and the slope of the line is $\Delta C_{p,obs}$ for the binding event. The $\Delta C_{p,obs}$ values for the binding of each compound were found to be identical within experimental error: **4**, -225 ($\pm$9); **6**, -213 ($\pm$17) cal mol^{-1} K^{-1} (Table 2). Hence, differences in the entropic contributions do not appear to arise from differences in solvation−desolvation or hydrophobic effects, but rather they are likely due to the preorganization and restriction of rotors by the cyclopropane. Because these values of $\Delta C_{p,obs}$ are very similar to that observed for the binding of an 8-mer pYEEI-containing peptide to this Src SH2 domain,[36] additional sequences at the *N*- or *C*-termini of the pYEEI motif do not appear to contribute significantly to $\Delta C_{p,obs}$.

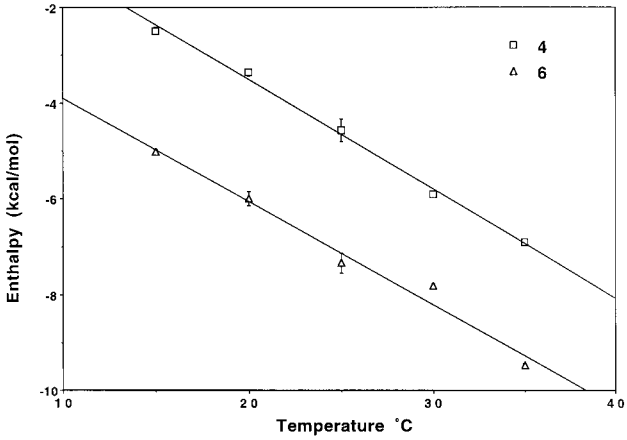

Figure 2. Temperature dependence of the binding enthalpy. ΔH_{obs} versus temperature was evaluated for compounds **4** (black square) and **6** (blue triangle). Error bars on the enthalpy values represent 95% confidence intervals. A linear least-squares best fit of the compounds **4** and **6** enthalpy data gives the heat capacity change for each compound, which are listed in the text and Table 2. The uncertainty in the heat capacity values represents a 95% confidence interval on the best linear fit.

Crystal Structure of the Src SH2 Domain−Compound 4 Complex. The difference of 1.4 kcal mol^{-1} in $\Delta H°_{obs}$ between compounds **4** and **6** suggested that these two compounds might bind to the Src SH2 domain differently. We therefore attempted to crystallize complexes of the Src SH2 domain with both compounds. Although crystals of a complex of the Src SH2 domain bound to compound **4** were readily obtained, we were unable to crystallize the Src SH2 domain bound to compound **6**. Data for the complex of **4** with the Src SH2 domain were collected to 1.9 Å resolution. Molecular replacement using a search model of the Src SH2 domain obtained previously was used to solve the structure that was subsequently refined to a

(56) Ladbury, J. E.; Lemmon, M. A.; Zhow, M.; Green, J.; Botfield, M. C.; Schlessinger, J. *Proc. Natl. Acad. Sci. U.S.A.* **1995**, *92*, 3199−3203.
(57) Lemmon, M. A.; Ladbury, J. E. *Biochemistry* **1994**, *33*, 5070−5076.
(58) Jencks, W. P.; Page, W. I. *Proc. Natl. Acad. Sci. U.S.A.* **1971**, *68*, 1678−1683.
(59) Williams, D. H.; Searle, M. S. *J. Am. Chem. Soc.* **1992**, *114*, 10690−10697.
(60) Robertson, A. D.; Murphy, K. P. *Chem. Rev.* **1997**, *97*, 1251−1267.
(61) Stites, W. E. *Chem. Rev.* **1997**, *97*, 1233−1250.

final R-factor of 23.6% and a final free R-factor of 26.7% (resolution range: 30−1.9 Å; $|F|/\sigma(F) > 2$). The crystals contained two molecules in the asymmetric unit, yielding two independent views of the complex of the Src SH2 domain and compound **4**. The two complexes align with an rms deviation of 1.5 Å for all protein atoms and 1.0 Å for backbone atoms. The ligands align with an rms deviation of 1.2 Å for all atoms. The significant deviation between the ligand structures in the two complexes is due to differences in side-chain conformations at the +1 and +2 position. When these side chains are excluded from the calculation, the rms deviation between ligand atoms is only 0.3 Å.

An overlay of the two structures from the asymmetric unit of the Src SH2 domain−**4** complex crystals is depicted in Figure 3A. A close-up overlay of the two bound structures of compound **4** is shown in Figure 3B. As shown in these figures, no significant differences are observed in the binding of the +3 Ile and pTyr residues between these two structures. The differences between the two complexes in the asymmetric unit of the crystal lie in the positioning of the first (+1 Glu) and second (+2 Glu) glutamate residues *C*-terminal to the pTyr in the ligand and in some of the residues in the protein interacting with the side chains of these two amino acids.

Differences between the two complexes at the +2 position are significant; in one molecule, the side chain of the +2 Glu interacts directly with Arg βD′1 (Figures 3A and 7), whereas in the second molecule, the +2 Glu side chain interacts with residues in a symmetry related molecule, and Arg βD′1 interacts instead with Thr BC3 in the pTyr-binding loop (the BC loop). In the crystal structure of the Src SH2 domain bound to an 11-mer peptide containing the pYEEI motif,[32] the +2 Glu was involved in stabilizing a water network extending to Arg βD′1 located 5 Å away. This water network was originally interpreted as important for determining the preferential recognition of Glu at the +2 position of the ligand by the Src SH2 domain.[30,32] In the two complexes of the Src SH2 domain bound to compound **4**, no such water network is observed.

The differences at the +1 Glu position are more localized and involve only the orientation of the Glu side chain of the ligand. Namely, the +1 Glu side chain of **4** adopts at least two different conformations as shown in Figure 3A and B, indicating that this side chain may interact weakly with the protein. From the interactions observed in the original crystal structure of the 11-mer peptide bound to the Src SH2 domain, it had been hypothesized that the Glu +1 side chain interacts specifically with the side chain of Lys βD3, which is the basic residue closest to the carboxylic group of +1 Glu. Interestingly, the conformation of Lys βD3 in this new structure is nearly identical in both complexes within the asymmetric unit, and the lysine ammonium group is directed toward a region of the Src SH2 domain that contains a patch of aspartate residues (Asp CD2 and Asp βC8) rather than toward +1 Glu (Figure 3C).

Comparison of Complexes of SH2 Domains with Rigidified and Flexible Ligands. Although the complex of the Src SH2 domain bound to the flexible peptide mimic **6** could not be crystallized, some qualitative insights regarding whether this flexible analogue binds in a mode different from the conformationally constrained peptide mimic may be drawn by comparing the structure of the complexes of the Src SH2 domain bound to compound **4** and to the 11-mer peptide that was reported previously.[32] This should be a valid comparison because only the four residues comprising the pTyr and the EEI sequence immediately *C*-terminal to pTyr made contact with the SH2 domain in the latter complex.[32] Hence, residues outside the pYEEI motif are not expected to significantly affect the conformation of the pYEEI sequence.

The crystal structure of the Src SH2 domain bound to the 11-mer peptide contained three complexes in the asymmetric unit, so three independent views of this complex were obtained.

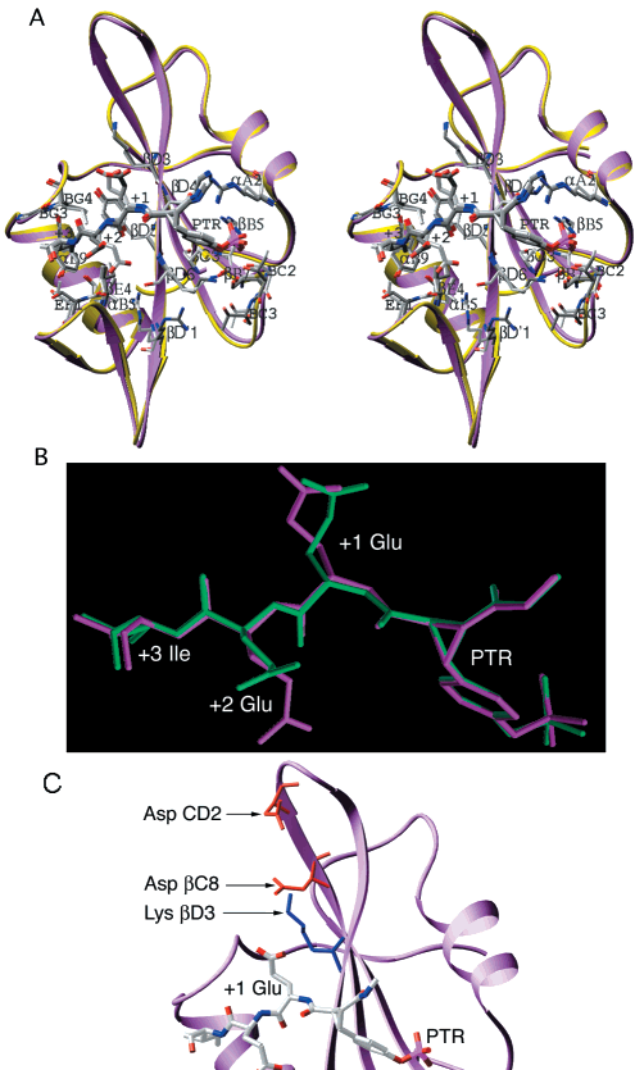

Figure 3. Superposition of the structures of the two Src SH2 domain−compound **4** complexes present in the asymmetric unit of the crystal. (A) Superposition of the two complexes. The protein backbone is shown in ribbon representation. The ligand and the residues of the protein involved in contacts with the ligand are shown in thick and thin ball-and-stick representation, respectively. The yellow and magenta protein ribbon models correspond to models 4.1 and 4.2 of Table 3, respectively. Color-coding for atoms in the ligand and the protein are the following: red for oxygen, blue for nitrogen, either light (model 4.1) or dark (model 4.2) gray for carbon, and pink for phosphorus. Protein residues are labeled according to previous convention.[32] Labeling of the pseudopeptide is PTR for the cyclopropane substituted phosphotyrosine, +1 for +1 Glu, +2 for +2 Glu, and +3 for +3 Ile. (B) Superposition of the two compound **4** structures from the two complexes in the asymmetric unit of the crystals. The structures corresponding to models 4.1 and 4.2 of Table 3 are shown in magenta and green, respectively. (C) Interaction of the Lys βD3 and Asp βC8 and Asp CD2. The pseudopeptide is represented as in (A). Lys βD3 is in blue, and the two aspartates are in red. The +1 position in the peptide is labeled +1 Glu, while the rigidified phosphotyrosine is labeled PTR.

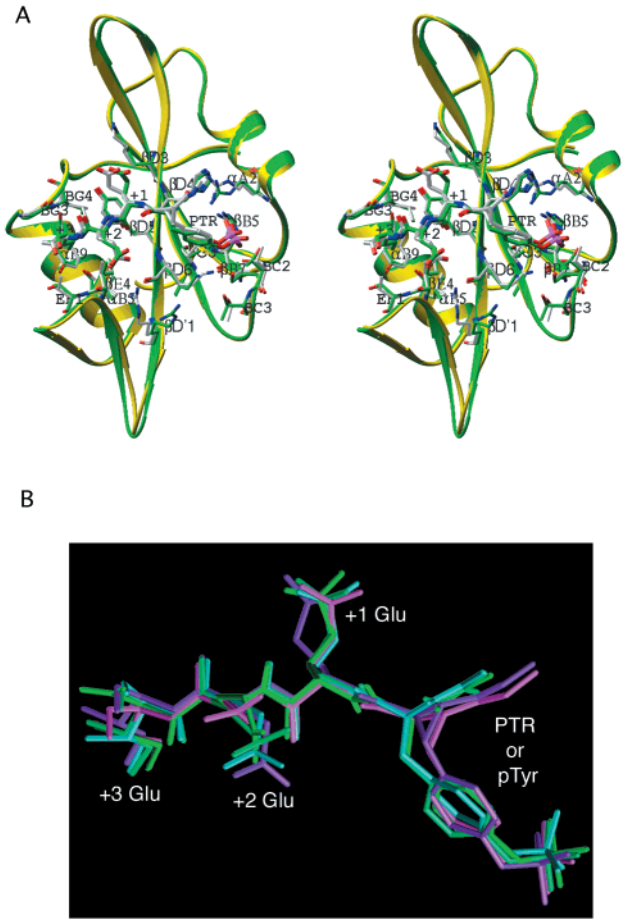

Figure 4. Superposition of the structures of one of the Src SH2 domain−compound **4** complex and one of the Src SH2 domain-11-mer flexible peptide described previously in Waksman et al.[32] (A) Superposition of the two complexes. Representation of the backbone structure and of the ligand is as in Figure 3A. The yellow and green ribbon models correspond to models 4.1 and 3.3 of Table 3. Color-coding for atoms in the ligand and the protein are as in Figure 3A except for carbons in model 3.3 which are in green. All residues in the protein are labeled according to Waksman et al.[32] Residues in the ligand are labeled PTR for the conformationally constrained phosphotyrosine, pTyr for the flexible phosphotyrosine of model 3.3, +1 for the +1 Glu, +2 for the +2 Glu, and +3 for the +3 Ile. (B) Overlay of the three bound structures of the 11-mer peptide (truncated for clarity to show only the pYEEI core) and the two conformations of **4** (purple and magenta).

A superimposition of these three ligand structures, together with those of the two Src SH2 domain−compound **4** complexes, is depicted in Figure 4B, while a superimposition of one of each of the two types of complexes is shown in Figure 4A. Inspection of these overlays reveals that there are no significant differences in the structures of the pTyr−+3 Ile segment in the backbones of **4** and the 11-mer peptide, and the orientations of these peptide backbones relative to the protein are essentially identical. The side chains of pTyr and Ile in the two ligands are also projected into their respective pockets of the SH2 domain in a nearly identical fashion.

For the purposes of the present study, it is significant that the spatial orientations of the carbonyl groups and the phosphate on the aromatic ring of the pTyr residue in the 11-mer peptide−SH2 domain complex are very similar to those of the corresponding substituents on the cyclopropane ring of **4** bound to the SH2 domain. The cyclopropane replacement in **4** thus serves as a reliable structural mimic of the bound conformation of the

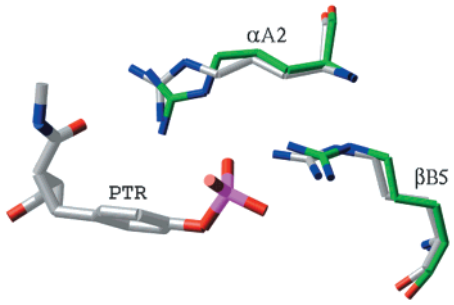

Figure 5. Arginine residues of the phosphotyrosine binding pocket; representation and labeling of residues in the peptide and in the protein are as in Figure 4A.

pTyr residue in SH2 domain binding ligands. The only significant differences found in the bound structures of **4** and the 11-mer peptide were in the orientations of the +1 and +2 Glu side chains. However, this is not surprising given that similar variations are observed in the orientations of these side chains of **4** and the 11-mer peptide in different complexes within asymmetric units.

The structures of the SH2 domain in each of these complexes are largely identical, but there is one notable difference in the pTyr binding pockets of the two. The constrained pTyr residue, labeled PTR, and the two Arg residues in the pTyr binding pocket, labeled Arg αA2 and Arg βB5, are depicted in Figure 5. The Arg residues in one of the complexes of **4** with the Src SH2 domain are shown in gray, while the Arg residues in one of the Src SH2 domain−11-mer peptide complexes reported previously are shown in green.[32] As is evident from Figure 5, the orientation of the guanidinium group in the side chain of Arg αA2 in the SH2 complex with **4** is flipped by approximately 180° relative to the complex with the 11-mer peptide; Arg βB5 remains unchanged in the two complexes.

This deviation in the conformation of the Arg αA2 side chain, which is consistent through the various structures within the asymmetric unit, may be significant because it results in a change in the hydrogen-bonding network within the complex. Namely, N^{ϵ} of Arg αA2 in the 11-mer peptide−SH2 domain complex forms a hydrogen bond with the phosphate group of pTyr, whereas in the SH2 domain complex with **4**, the N^{ϵ} of Arg αA2 is directed away from the phosphate moiety making instead a hydrogen bond with a water molecule. Since the net number of hydrogen bonds is maintained, the impact of the change in Arg αA2 side-chain conformation upon binding affinity cannot be easily predicted.[62] Another possible consequence of the different orientation of the Arg αA2 side chain in the SH2 domain−**4** complex is the disruption of a π-cation interaction with the tyrosine ring, which had been observed in the Src SH2 domain−11-mer peptide complex structure,[32] because the distance between the guanidine nitrogen closest to the centroid of the tyrosine ring has increased to 3.8 from 3.3 Å in the original complex.

Several other conformational aspects of the bound structure of **4** are noteworthy. For example, the amide carbonyl group that links the pTyr to the +1 Glu bisects the cyclopropane ring, whereas the carbonyl group of the *N*-terminal methyl amide is deflected from this bisecting orientation by approximately 30° (Figure 6). Structural and conformational studies of cyclopropyl

(62) Fersht, A. R. *Trends Biochem. Sci.* **1987**, *12*, 301−304.

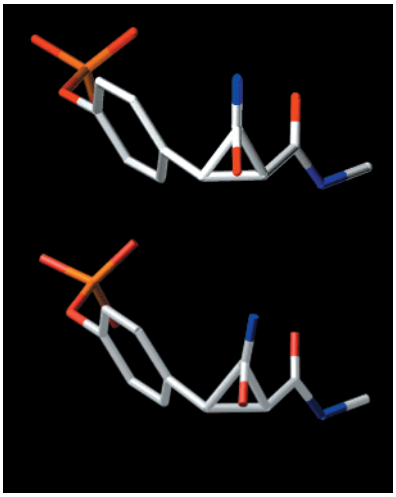

Figure 6. Conformation of the carbonyl group of cyclopropane-rigidified phosphotyrosine (B); representation and labeling of residues in the peptide and in the protein are as in Figure 4A. The top panel represents the bisecting orientation of the pTyr-+1 Glu amide carbonyl, while the lower panel represents the significant deviation from the "preferred" bisecting orientation of the methylamide-pTyr carbonyl that is observed in the crystal structure.

carbonyl compounds suggest that the preferred orientation of the carbonyl group is the one in which the carbon−oxygen double bond bisects the cyclopropane ring.[63−66] Indeed, we have observed this preference in the crystal structures of several cyclopropane-derived peptide mimics,[67] including the trisubstituted cyclopropane subunit in **4** (see Supporting Information). We have previously observed similar deviations from this "ideal" bisecting conformation in earlier structural studies of free and bound cyclopropane-containing inhibitors of HIV protease,[16] so the energetic consequences of such small torsional changes are difficult to predict. The methyl group of the *N*-terminal amide is also rotated out of the plane of the carbonyl group by approximately 22°. This deviation from planarity, which results in the loss of some amide resonance, may result from a steric interaction with a guanidinium nitrogen of Arg αA2 only 3.3 Å away (Figure 7).

Surface Area Calculation and Derivation of Thermodynamic Parameters from Structure. Despite the overall similarities in the putative binding modes of compounds **4** and **6**, the introduction of a cyclopropane ring in **4** could result in differences in surface contact areas that might help explain the observed differences in binding enthalpy. To address this question, the structure of the pYEEI core of the 11-mer peptide was used to generate two models.[32] In the first one, the *N*-terminal amino group of the pYEEI peptide was acetylated to constitute compound **3**. In the other model, a CH_3-$NHCOCH_2$− moiety was substituted for the amino group on the Cα atom of pTyr to give compound **6**, and this structural subunit of **6** was then manually oriented into a conformation that corresponded to that of the trisubstituted cyclopropane in the SH2 domain−**4** complex. These models were then minimized using conjugate gradient protocols. Polar and nonpolar contact surface areas were calculated for **4**, **6**, and **3** using the

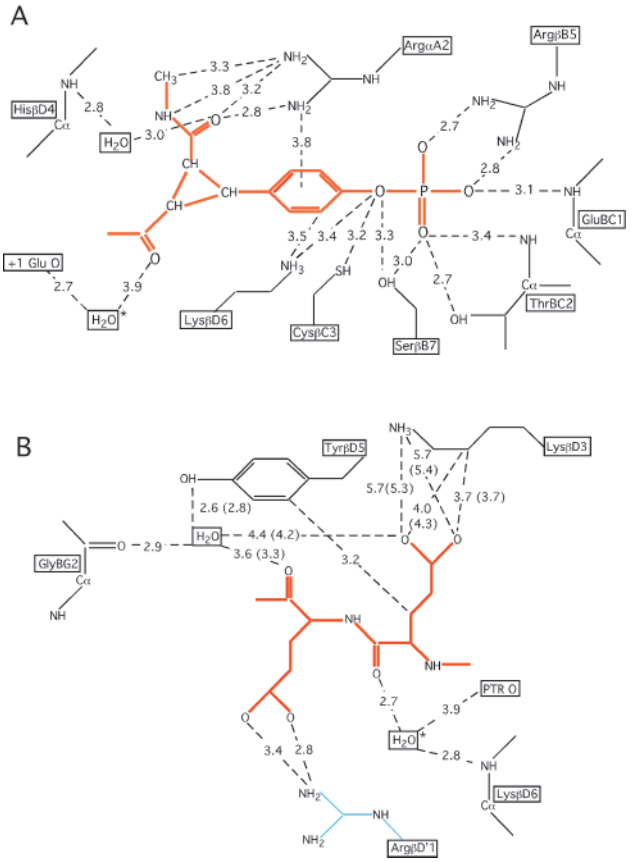

Figure 7. Schematic diagram of the interactions between the rigidified phosphotyrosine and the pTyr binding pocket (A) and between the +1 and +2 positions and the protein (B). Schematic drawings of the ligand and protein residues are indicated in thick red and thin black lines, respectively. Dashed lines connect atoms of the ligand and the protein that are within contact distances. Numbers on the dashed lines indicate corresponding distances. In (B), PTR indicates the conformationally constrained phosphotyrosine, and "PTR O" indicates the carbonyl oxygen of PTR. Arg βD′1 is in light blue, because its guanidinium group is observed in contact with the +2 Glu in only one molecule in the asymmetric unit crystal. In (A) and (B), * labels the same water molecule.

method described above (see Experimental Section), the thermodynamic parameters were computed,[52,54] and the results are summarized in Table 3.

This computational method has been applied successfully in a number of studies involving the prediction of binding energetics of protein−peptide or protein−protein interactions.[68−70] However, in the present instance, these calculations do not predict accurately the observed energetic parameters for the binding of phosphotyrosyl peptides to SH2 domains. For example, the calculated free energy for the binding of compound **3**, a tetrapeptide, varies between −7.3 and −4.3 kcal mol^{-1}, a value that compares poorly against the experimentally determined value of −9.0 kcal mol^{-1}. There is also a striking lack of convergence among the predicted thermodynamic values derived from equivalent structures. For example, the free energy of binding of compound **4** calculated from one structure in the asymmetric unit yields a free energy of −11.3 kcal mol^{-1}, whereas the same calculation using the other structure for the complex yields the very different value of −6.2 kcal mol^{-1}.

(63) Allen, F. H. *Acta Crystallogr., Sect. B* **1979**, *36*, 81−96.
(64) Allen, F. H. *Acta Crystallogr., Sect. B* **1981**, *37*, 890−900.
(65) Allen, F. H.; Kennard, O.; Taylor, R. *Acc. Chem. Res.* **1983**, *16*, 146−153.
(66) de Meijere, A. *Angew. Chem., Int. Ed. Engl.* **1979**, *18*, 809−886.
(67) Lynch, V. M.; Austin, R. E.; Martin, S. F.; George, T. *Acta Crystallogr., Sect. C* **1991**, *47*, 1345−1347.
(68) Baker, B. M.; Murphy, K. P. *J. Mol. Biol.* **1997**, *268*, 557−569.
(69) Gomez, J.; Freire, E. *J. Mol. Biol.* **1995**, *252*, 337−350.
(70) Murphy, K. P.; Xie, D.; Garcia, K. C.; Amzel, L. M.; Freire, E. *Proteins* **1993**, *15*, 113−120.

Table 3. Calculated Binding Energies of the Src SH2 Domain Interaction with Compounds **4**, **3**, and **6**[a]

model	ΔASA total (Å)	ΔASA polar (Å)	ΔASA nonpolar (Å)	$\Delta C^\circ_{p,calc}$ cal/mol/K	ΔH°_{calc} kcal/mol	ΔS°_{solv} cal/mol/K	ΔS°_{conf} cal/mol/K	ΔS°_{calc} cal/mol/K	ΔG°_{calc} kcal/mol
4.1	−989	−521	−468	−105.1	−15.5	27.0	−32.9	−13.8	−11.3
4.2	−948	−477	−471	−84.8	−13.4	21.7	−37.9	−24.0	−6.2
3.1	−963	−470	−493	−76.0	−12.8	19.4	−39.9	−28.3	−4.3
3.2	−967	−504	−462	−99.1	−14.8	25.3	−42.6	−25.1	−7.3
3.3	−1001	−494	−507	−83.1	−13.6	21.2	−41.1	−27.7	−5.3
6.1	−970	−500	−469	−95.4	−14.5	24.4	−29.0	−28.3	−10.8
6.2	−1010	−516	−494	−95.8	−14.2	24.5	−44.1	−27.4	−6.6
6.3	−1032	−488	−543	−70.8	−12.7	18.0	−36.8	−27.7	−4.8

[a] Surface area calculations and derivation of binding energetics were carried out as described in the Experimental Section. Model 4.1 and 4.2 refer to the two experimental Src SH2 domain structures bound to compounds **4** present in the asymmetric unit of the crystal. Models 3.1, 3.2, and 3.3 refer to the structures of the Src SH2 domain bound to compound **3** (Figure 1B). Here, the starting structures for modeling compound **3** were those of the three Src SH2 domain-11-mer peptide complexes determined previously.[32] Models 6.1, 6.2, and 6.3 refer to the structures of the Src SH2 domain bound to compound **6** (Figure 1B). The starting structures of these models were as for models 3.1, 3.2, and 3.3.

The range of calculated free energy values is narrower for compound **3**, but it is still unusually large. Similarly, the calculated enthalpy and entropy changes do not correlate well with the experimental values (Tables 2 and 3). It is perhaps significant that even though the calculated values for ΔS for the conformationally constrained pseudopeptide **4** are very different (−13.9 and −24.0 cal mol^{-1} K^{-1}), they are less negative than for the more flexible compounds **6** and **3**.

Discussion

Introducing conformational constraints into a flexible ligand to enforce or stabilize its bound structure has been widely used as a strategy for the design of new ligands that will have higher affinity for a selected macromolecular target. The rationale for this method is straightforward: reducing the conformational entropic penalty that must be paid upon binding would be predicted to result in a net gain in the free energy of binding provided all favorable binding interactions remain and no unfavorable steric contacts are introduced. While there are a number of examples that support this hypothesis,[1−7] there have been no reports of detailed thermodynamic studies using a structurally well-characterized biological system.

We have used cyclopropanes as dipeptide replacements in designing a number of conformationally constrained enzyme inhibitors having high potencies.[15−17,19,20,34] In the present study, 1,2,3-trisubstituted cyclopropanes were prepared to replace the Cα, Cβ, and amide nitrogen of a phosphotyrosine residue in the pYEEI tetrapeptide **3**, which is a ligand for the SH2 domain of the Src kinase. These substitutions led to the pseudopeptides **4** and **5** in which the phosphotyrosine side chain and backbone were constrained in an orientation that modeling had suggested would closely mimic that of a pTyr residue bound to the Src SH2 domain. The effects of thus rigidifying the pTyr subunit of pYEEI upon binding to the Src SH2 domain were examined using calorimetry and X-ray crystallography. The thermodynamic parameters, ΔH°, ΔS°, ΔG°, were obtained for complex formation between the Src SH2 domain and compounds **3**−**7**, and the ΔC_p of binding for the conformationally constrained pseudopeptide **4** and its flexible analogue **6** was determined. These binding parameters were then interpreted in light of crystal structures of the complexes of the Src SH2 domain with **4** and with a natural 11-mer peptide.

Constraining the pTyr of **3** with a substituted cyclopropane replacement had the expected beneficial effect upon the observed ΔS° as the binding of **4** and **5** to the Src SH2 domain was entropically favored over **6** and **7** by 5−9 cal mol^{-1} K^{-1}. This result supports the hypothesis that the preorganization of a ligand in its active conformation gives rise to an entropic advantage in binding to its biological target. Entropies of internal rotations in the gas phase are known experimentally, and they appear to be similar in solution.[58,71] For example, the loss of two rotational rotors has been estimated to be 7−8 cal mol^{-1} K^{-1} at 298 K.[58,71] This value corresponds to that predicted for the restriction of the two rotors about the χ_1 and Φ angles by introducing the 1,2,3-trisubstituted cyclopropane ring (Figure 1B). Hence, in the present instances, the experimental results agree with predictions.

This study reveals a number of important and interesting features regarding the use of substituted cyclopropanes in the design of conformationally constrained phosphopeptide inhibitors having high affinity for the Src SH2 domain. Introducing a cyclopropane as a conformational constraint into compounds **4** and **5** did have the expected effect upon the entropy of binding, but the constrained (**4**, **5**) and flexible analogues (**6**, **7**) had comparable binding affinities for the Src SH2 domain because the favorable gain in entropy was compensated by an unfavorable enthalpic change. We have shown through cocrystallization with the Src SH2 domain that the binding modes of compound **4** and an 11-mer peptide containing the pYEEI sequence do not differ. Superimposition of these two complexes does not reveal dramatic changes in the way the pseudopeptide and the peptide are bound. The bound structures of the ligands are similar, and both ligands make comparable interactions with the protein. Including the differing conformations observed in Arg αA2 and the slight deviations observed around the phosphotyrosine, the differences in contacts between the two ligands and the SH2 domain are qualitatively no greater than the differences observed between similar complex structures in the asymmetric units of the crystals. A computational study of the binding interface between the pYEEI core of the 11-mer peptide (i.e., **3**), **4**, and **6** and the Src SH2 domain did not reveal any significant differences in either the mode of ligand binding or the buried accessible surface area. Hence, although the slight deviations observed may influence the enthalpy term unfavorably, it is not possible to assign a value to the individual contributions, and the underlying causes for the observed difference in enthalpy contribution between ligands remain unclear.

A large body of data has been accumulated on recognition and binding of tyrosyl phosphopeptides by the Src SH2

(71) Williams, D. H.; Gerhard, U.; Searle, M. S. *Bioorg. Med. Chem. Lett.* **1993**, *3*, 803−808.

domain.[36−39,41,43] All of these data underscore the difficulty of interpreting thermodynamic parameters in light of structure. In a recent study, about 30 Src SH2 domain mutants containing alanine substitutions were examined in an attempt to correlate the structural changes that accompany these mutations with variations in the thermodynamic parameters $\Delta G°$, $\Delta H°$, and $T\Delta S°$. The van der Waals contacts and buried surface areas upon removal of a side chain were examined, and no correlation could be established.[37] Similar conclusions were drawn from a much more exhaustive study by Henriques et al.[43] who attempted to predict thermodynamic parameters from a number of known structures of complexes of the Src SH2 domain.[43] Five different area-based models were tested in which ligand conformational flexibility and proximal ordered solvent molecules were treated in various ways in the surface area calculations. None of these models predicted the thermodynamic parameters for binding of a pYEEI-containing peptide to the Src SH2 domain with any degree of accuracy. In the present study, a similar computational method not only failed to predict any of the thermodynamic binding parameters, but there was also a striking lack of convergence among the predicted thermodynamic values derived from several similar complexes of an asymmetric unit of the crystal. Such discrepancies may be caused by slight but cumulative differences between complexes in the asymmetric unit. These differences probably arise from packing forces that can disturb side-chain orientations and local structures at and around the crystal packing interfaces. Hence, the present work further illustrates the deficiencies in existing computational methods for predicting binding of phosphotyrosine-containing peptides by SH2 domains.

The crystal structure of the Src SH2 domain bound to the constrained pseudopeptide **4** further illuminates the roles of some of the side chains in binding. Although the structures described here are very similar to those already reported,[32] there are some small, yet likely significant, differences. Previous studies have shown that, among the four ligand residues involved in binding, the pTyr and the +3 Ile contribute most to the free energy of binding.[39,40] This finding is consistent with the two-pronged model of SH2 domain binding and is reflected in the fact that in all structures of the Src SH2 domain bound to a pYEEI peptide, little variation in structure around the pTyr and the +3 Ile is observed.[32] Most of the structural variations observed in the ligands are localized around the +1 and +2 positions and in the water structure surrounding the +2 position, suggesting that these side chains contribute only modestly to binding.[39]

Deviations in the +1 Glu side-chain orientations observed in the cocrystal structure described here confirm a previous study that showed that mutating the +1 Glu position in the ligand to Ala has little impact on the binding of a pYEEI-containing peptide.[39] It was originally hypothesized that the carboxyl group of +1 Glu interacted favorably with the side chain of Lys βD3, located nearby on the surface of the SH2 domain.[32] However, the crystal structure described here suggests another role: Lys βD3 appears to balance other surface charges presented by a cluster of aspartate carboxyl groups, Asp CD2 and Asp βC8 (Figure 3C). It has been shown that mutating Lys βD3 to Ala results in a significant drop in the free energy of binding, presumably due to the repulsion that the cluster of aspartate carboxyl groups on the SH2 domain exerts on the +1 Glu position of the peptide.[37] Hence, the role of Lys βD3 in pYEEI peptide binding may be to neutralize the negative charge of this cluster of carboxylic groups.

The binding of the +2 Glu was originally thought to be influenced by a water network bridging the +2 Glu carboxyl group to Arg βD′1,[32] and other studies have also claimed a role for this water network.[72] However, when Arg βD′1 of the SH2 domain was mutated to either Phe or Ala, there was only a very small loss in binding free energy of 0.3 kcal mol^{-1} for Phe βD′1 and 0.6 kcal mol^{-1} for Ala βD′1.[37] This observation suggested that the water-network-mediating interactions between +2 Glu and Arg βD′1 reported by Waksman et al.[32] may not play a critical role in determining selectivity at the +2 position. This conclusion is supported by the new crystal structure presented herein where there are no such bridging water networks between the βD′1 position in the protein and the +2 position in the ligand.

Because the structures of the complex of **4** with the Src SH2 domain are of high resolution, the solvent substructure around the complex and within the interface was defined with precision. Two water molecules are found at the ligand−protein binding interface, and by the nature of the interactions these make, both the protein and the ligand indicate that they may play an important role in binding (Figure 7). Both of these waters are involved in extensive hydrogen-bonding interactions with the ligand and the Src SH2 domain. The first water molecule, which is labeled with an asterisk (*) in Figure 7, lies near the conformationally constrained pTyr group (indicated as PTR) and +1 Glu. This water makes H-bond interactions with the *N*-terminal carbonyl oxygen of pTyr (or PTR), the carbonyl group of the +1 Glu, and the amide nitrogen of Lys βD6. The second water molecule in Figure 7B is positioned between the +2 Glu and +3 Ile. It also is hydrogen bonded with the carbonyl oxygen of +2 Glu, with the carbonyl oxygen of Gly BG2 in the BG loop, and with the terminal hydroxyl of the side chain of Tyr βD5. These hydrogen bonds, notably the one with the hydroxyl group of Tyr βD5, were not observed previously.[31,32] Tyr βD5 has been identified previously as one of the two hotspot residues in the binding interface of the Src SH2 domain. Tyr βD5 appears to play several roles at this interface. It forms a portion of the hydrophobic +3 Ile-binding cavity, the so-called +3 binding pocket where the +3 Ile of the pYEEI peptide inserts.[37] It also forms a van der Waals contact with the Cβ of the +1 position residue as well as a platform for the backbone of the phosphoryl peptide ligand.[32] The structures of the Src SH2 domain−compound **4** complex suggest that Tyr βD5 may play an additional role in anchoring the BG loop to the ligand backbone through the involvement of a water molecule. In any case, it is interesting to note that the water structure around the binding site implicates mostly main chain atoms in the ligand and therefore is not expected to play a role in determining the specificity of the phosphopeptide−SH2 domain interaction.

This study reveals a number of important and interesting features regarding the design and evaluation of conformationally constrained peptide mimics. Clearly there is an entropic advantage that accompanies restricting the number of rotatable bonds in closely related peptide-like ligands as evidenced by the favorable change in $\Delta S°$ for **4** relative to **6**. This observation

(72) Chung, E.; Henriques, D.; Renzoni, D.; Zvelebil, M.; Bradshaw, J. M.; Waksman, G.; Robinson, C. V.; Ladbury, J. E. *Struct. Fold. Des.* **1998**, *6*, 1141−1151.

validates one of the original premises that led to the invention and use of 1,2,3-trisubstituted cyclopropanes as rigid replacements of extended peptide secondary structure. However, this entropic advantage was unexpectedly compensated by a loss in binding enthalpy. Entropy−enthalpy compensation, which involves corresponding changes in $\Delta H°$ and $\Delta S°$ so that the changes in $\Delta G°$ are minimized, is beginning to appear as a general phenomenon in interactions of proteins with peptides and peptide-like ligands.[73,74] The similarity of the crystal structures of the Src SH2 domain with the conformationally constrained pseudopeptide **4** and an 11-mer peptide coupled with the magnitudes of the deviations in $\Delta H°$ and $\Delta S°$ between the flexible and cyclopropane-containing ligands in this study convincingly demonstrate that complete thermodynamic profiles and structural data must be obtained to evaluate the consequences of introducing a conformational constraint into a molecule. Developing a paradigm for designing high-affinity ligands so that favorable enthalpic interactions are maintained while minimizing the unfavorable entropy of binding will be a major challenge for the future.

(73) Sharp, K. *Protein Sci.* **2001**, *10*, 661−667.
(74) Liu, L.; Guo, Q.-X. *Chem. Rev.* **2001**, *101*, 673−695.

Acknowledgment. This work was funded by NIH grants GM60231 (to G.W.) and GM43473 (to S.F.M.) and by The Robert A. Welch Foundation (to S.F.M.) and the Texas Advanced Research Program (to S.F.M.). J.P.D. and O.L. contributed equally to this work.

Supporting Information Available: Complete experimental details and characterization (^{1}H and ^{13}C NMR spectra, IR spectra, and mass spectra) of **3**−**7** and all new compounds leading to their synthesis together with X-ray crystal structural data for the cyclopropyl pTyr replacement in **4** (PDF). This material is available free of charge via the Internet at http://pubs.acs.org.

JA011746F